



# A novel modeling method for soil water retention curve considering soil deformation and its application

Haiman Wang<sup>1,2</sup> · Wankui Ni<sup>1,2</sup> · Kangze Yuan<sup>1,2</sup>

Received: 15 October 2022 / Accepted: 27 April 2023 / Published online: 12 June 2023  
© The Author(s), under exclusive licence to Springer-Verlag GmbH Germany, part of Springer Nature 2023

## Abstract

Soil water retention curves (SWRC) are commonly used to predict unsaturated infiltration coefficients, but the conditions studied in traditional SWRC models are mostly isochoric conditions. It is assumed that there is a coupling function linking changes in water ratio with changes in void ratio, and that the coupling function depends on soil saturation under constant suction conditions. Based on the above assumptions the void ratio is introduced into the SWRC model and a SWRC for deformed soils is established. The two parameters added to the new model can be determined by constant suction compression tests. The final model for predicting the unsaturated permeability coefficient of deformed soils was obtained based on the SWRC discretization. The unsaturated permeability coefficient prediction model has only one additional parameter compared to the SWRC model and the parameter is a constant for the same soil and can be obtained from simple saturated permeability tests. Finally, the reliability of the model for application in the compacted loess of Yan'an was verified by means of a self-designed device for water infiltration.

**Keywords** Loess · Suction · Soil water retention curve · Unsaturated permeability coefficient

## Introduction

The permeability coefficient and seepage law of soil are important topics in soil mechanics and geotechnical engineering. Since the unsaturated permeability coefficient is closely related to the SWRC, establishing the relationship between the unsaturated permeability coefficient and the SWRC can serve the purpose of predicting the unsaturated permeability coefficient from the SWRC. Therefore, studying the permeability coefficient and SWRC has both theoretical and practical significance.

SWRCs are the key to describing the seepage, mechanics and their coupling processes in unsaturated soils (Hu et al. 2013). The work done so far on the SWRC is very large (Leong 2019). The traditional SWRC models assume a simple relationship between the degree of saturation and suction, mostly without considering the effect of deformation (Beckett and Augarde 2013; Fredlund and Xing 1994; van Genuchten 1980). However, as the study progressed, water retention was also influenced by the pore structure (Frydman and Baker 2009; Gens et al. 2011; Iyer et al. 2018, 2019; Otalvaro et al. 2016; Romero and Jommi 2008). For small deformation it is acceptable to ignore the deformation of the specimen. However, for some special soil (loess) in the water content changes will produce larger deformation (collapse), in this case the soil deformation cannot be ignored. For this reason, some scholars have experimentally studied the evolution of SWRC due to structural changes in soils under different conditions, such as drying and wetting cycles and shrinkage (Wen et al. 2020, 2021b; Zhao et al. 2020). However, the SWRC measurements are time consuming. This is because it takes a long time for the pore water to reach stability in the soil under each matric suction. For this reason, the researchers introduced the void ratio based on the original model and described the influence of the combined

✉ Wankui Ni  
18700425209@163.com; niwankui@chd.edu.cn

Haiman Wang  
2020026006@chd.edu.cn

<sup>1</sup> College of Geological Engineering and Geomatics, Chang'an University, Xi'an 710054, Shaanxi, People's Republic of China

<sup>2</sup> Key Lab of Western Geological Resources and Geoengineering Under Ministry of Education, Chang'an University, Xi'an 710054, Shaanxi, People's Republic of China

effect of the void ratio and the matric suction on the degree of saturation (Gallipoli et al. 2003; Mašín 2010; Nuth and Laloui 2008; Pasha Amin et al. 2016; Da et al. 2007; Zhou et al. 2012). The above-mentioned SWRCs considering deformation can be broadly classified into two categories. The first category considers that the effect of deformation on the SWRC is reflected by the air-entry value (Nuth and Laloui 2008). The effect of deformation on the SWRC was reflected by establishing the relationship between the void ratio and the air entry value (Huang et al. 1998), and the results of the study showed that the air entry value is a power function of the void ratio (Gallipoli 2012, 2003). The second type is the SWRC model established with the aid of theoretical analysis on the basis of experiments. Based on the experimental results, a relationship between water content and suction was established to introduce the void ratio into the SWRC model (Mašín 2010; Da et al. 2007). Theoretical analysis of the saturation variation process under the condition of three-phase proportional constraint predicted by the dual influence of void ratio and suction (Zhou et al. 2012).

The main ways to obtain the unsaturated permeability coefficient are direct measurement and estimation using models. The direct measurement of permeability coefficient requires special testing equipment and the technical requirements are high (Wen et al. 2019, 2022). Therefore, various models have been proposed to estimate the permeability coefficient, using the relatively easy to measure water holding capacity (Fredlund and Xing 1994; Gardner 1958; Gui and Hsu 2009; Hunt et al. 2013; Lebeau and Konrad 2010; van Genuchten 1980; Wen et al. 2021a). For prediction of permeability coefficients of deformed soils, empirical prediction methods are mostly used (Reicosky et al. 1981), i.e., an empirical formula is obtained by a large number of statistics. However, the structure between different soils has obvious differences, and the applicability of the empirical formula has great limitations. SWRC can be used to predict the unsaturated permeability coefficient of soils. Fredlund and Xing (1994) proposed a permeability coefficient function built on the SWRC. Agus et al. (2005) proposed a method for estimation of permeability functions (i.e., saturated and unsaturated permeability coefficients) using SWRCs and saturated permeability coefficients obtained in the laboratory for some residual soils in Singapore. Tao et al. (2019) proposed a prediction method for unsaturated permeability coefficients based on the concept of differential SWRCs by combining the theory of fluid dynamics. The above research results fully demonstrate the feasibility of predicting unsaturated permeability coefficients by SWRCs, but the above research results are conducted under constant volume conditions. Therefore, the above methods do not consider the effect of deformation on the unsaturated permeability coefficient.

Theoretical studies based on both the SWRC model under deformation conditions and the prediction of unsaturated permeability coefficient by SWRCs can be obtained for the prediction model of unsaturated permeability coefficient under deformation conditions. Based on the above concept this study extends the traditional isovolume SWRC model to deformation conditions by introducing the void ratio, and then establishes the unsaturated permeability coefficient prediction model under deformation conditions with the help of the SWRC model under deformation conditions. The reliability of the model was finally verified by the data obtained from the home-made instrument.

## Materials and methods

### Test device

A homemade one-dimensional instantaneous infiltration device was used to measure the unsaturated permeability and SWRCs in this study, as shown in Fig. 1. The infiltration device mainly consists of a test bench, plexiglass barrel, vertical loading device, moisture sensor, water potential sensor, and data acquisition system. In addition to fixing the Plexiglas barrel and the vertical loading device, the test bench can also adjust the distance between the Plexiglas barrel and the vertical loading device. The plexiglass barrel was 63 cm high; the inner diameter was 30 cm; and the barrel wall thickness was 1 cm. Its lateral deformation is less than 0.02% after the vertical load is applied, which is negligible. Plexiglas barrels on both sides of the vertical spacing of 10 cm evenly distributed small holes of 0.8 cm in diameter. The EC-5 moisture and MPS-6 water potential sensors are installed in the small holes on each side. MPS-6 water potential sensor developed by the United States METER company, the measurement range of 9–100000 kPa; resolution of 0.1 kPa; measurement accuracy of 2 kPa; measurement time of 150 ms. The EC-5 moisture sensor has a range of 0–100%; resolution of 0.1%; measurement accuracy of 3%; and measurement time of 10 ms. The vertical loading device is mainly used for compacting the soil inside the Plexiglas barrel. The Plexiglas barrel is tightly fixed to the steel base by 4 threaded tie rods during the test. The base of the soil column is evenly distributed with 5 mm diameter permeable holes, under which is a water collection tank to drain water through a drainage pipe.

### Materials

The loess used in this study was sampled in Yan'an New District, and the soil at the sampling site was  $Q_3$  loess. To minimize sampling disturbance, all the samples were retrieved by hand, sealed with a plastic film inside a cylindrical iron

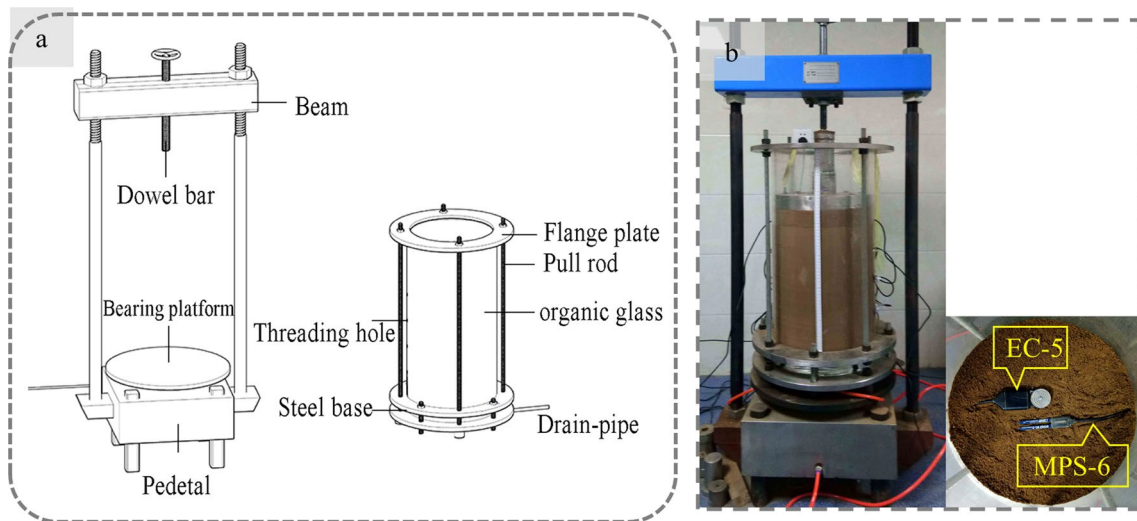


Fig. 1 Self-made unsaturated permeating instrument. a Schematic; b Physical image

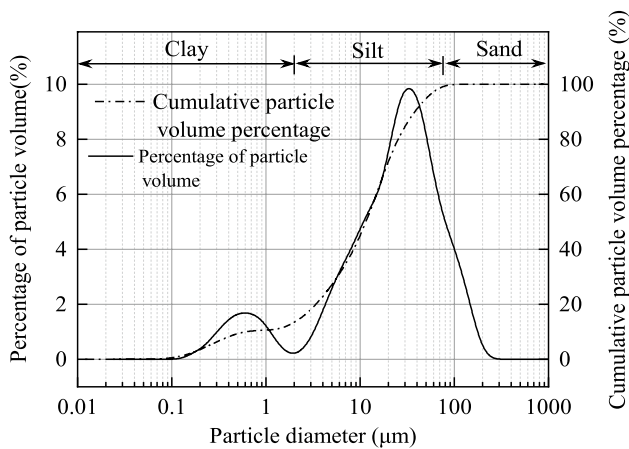


Fig. 2 Particle size distribution of the tested loess

bucket, and transported to the laboratory. The physical properties of the retrieved material were determined following ASTM test methods. The particle size distribution was tested by a Battersize 2000 laser particle size distribution meter, which showed that the loess sample consisted mainly of powder particles (about 78.99%), with approximately the same sand and clay content of 10.39% and 10.62%, respectively (Fig. 2). Physical parameters, Atterberg limits, and the particle size distribution of the loess samples are listed in Table 1.

**SWRCs and unsaturated permeability tests**

Previous studies have shown that SWRC is largely controlled by soil microstructure (Li et al. 2018; Mu et al. 2020; Muñoz-Castelblanco et al. 2012; Ng et al. 2016). The prepared sample water content influences the pore size

Table 1 Major physical properties of the loess used in this study

Property	Value
Maximum dry density $\rho_d$ (g/cm <sup>3</sup> )	1.69
Natural water content $w$ (%)	10.19
Specific gravity $G_s$	2.72
Liquid limit $w_L$ (%)	28.9
Plastic limit $w_p$ (%)	16.1
Particle size distribution	
Sand 0.075–2 mm (%)	10.39
Silt 0.002–0.075 mm (%)	78.99
Clay <0.002 mm (%)	10.62

distribution curve of loess (Monroy et al. 2010; Oualmakran et al. 2016). From Table 1, the natural water content of loess is 10.19%. To make the microstructure of the specimens close to the natural loess to the maximum extent, the water content was set to 10%. The specimen preparation process is as follows. The soil samples were air-dried by knocking with a rubber hammer, passed through a 2 mm sieve and configured with a loose soil of 10% water content. Loose soil was loaded into the incubator to allow sufficient water uniformity for sample preparation. Based on the water content of the soil, the cross-sectional area of the Plexiglas bucket and the target dry density, the mass of soil required for a 5-cm high soil column was calculated. The soil of the corresponding quality is evenly spread in the glass bucket, and then the loose soil is compacted to a height of 5 cm with the pressure device that comes with the infiltration device. During the compaction process, the virtual soil is uniformly stressed. Repeat the above steps to compact the soil in layers and shave the interface between the soil layers. The final soil columns with a height of 50 cm and dry densities of 1.45, 1.55

and 1.65 g/cm<sup>3</sup> were made. MPS-6 water potential sensors and EC-5 moisture sensors were placed in the hole running up both sides of the barrel. One set of sensors was set every 10 cm, and a total of four sets were placed. A 10 cm thick glass bead was placed on the upper part of the soil column to prevent compaction of the soil surface or water seepage along the sidewall during the simulated rainfall process. A water spray can be used to simulate rainfall, and the total spraying time was 30 min, with a total rainfall of 4400 ml. Immediately after the rainfall, the top of the soil column was sealed with plastic wrap to prevent water from evaporating. Because the plexiglass barrel is transparent, the entire moisture infiltration process can be clearly observed, and the sensors record water potential and moisture data in real time. SWRC can be plotted based on the moisture and water potential recorded by the sensor. In addition, the unsaturated permeability coefficient of the specimen at different saturations (matric suction) can be calculated by the instantaneous profile method based on the variation of moisture and water potential with time at different locations of the soil column.

### Saturated permeability test

A metal mold is employed for statically compacted soil. The dry density of the specimens was 1.45, 1.55, and 1.65 g/cm<sup>3</sup>, respectively. The dry density of the specimens used for saturated permeability and the soil columns used for unsaturated permeability tests were kept consistent. Therefore, the results of the saturation permeability test can be used to determine the saturation permeability of the soil column. The variable head method measured the saturation permeability at 20 ± 2 °C. Nanjing Soil Instrument Factory produced the instrument used in this study (Fig. 3). The specific operation steps were reported in Yuan et al. (2022). The variable head permeability was determined using the following formula:

$$K_s = 2.3 \frac{aL}{A(t_2 - t_1)} \log \frac{H_1}{H_2} \tag{1}$$

where  $k_s$  is the permeability (cm/s),  $A$  is the cross-sectional area of the sample (cm<sup>2</sup>),  $a$  is the cross-sectional area of the tube (cm<sup>2</sup>),  $L$  is the height of the sample (cm), and  $t_1$  and  $t_2$  are the start and end times of the test (s), respectively.

### Model building

#### SWRC model considering deformation

The pore ratio  $e$  (i.e., pore volume per unit solid volume) under constant suction may cause a change in the response of the water ratio  $e_w$  (i.e., water volume per unit solid volume),

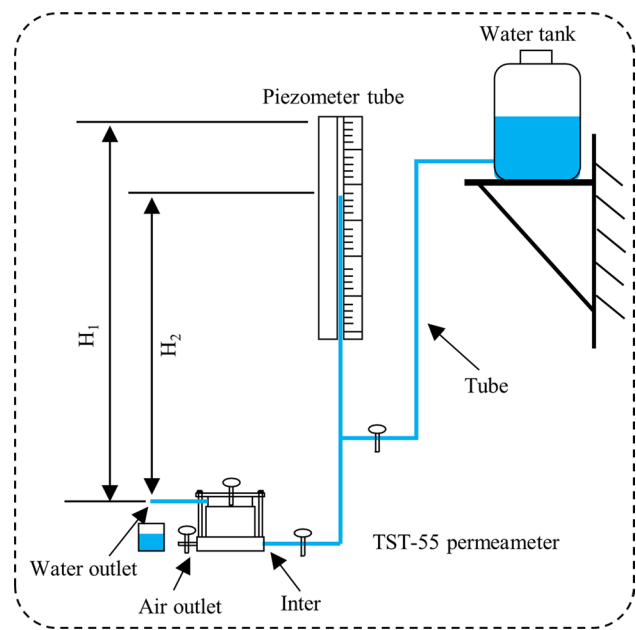


Fig. 3 Saturated permeation test device

the magnitude of which depends on the amount of deformation of the pores filled or potentially filled with water. It can be assumed that the change in pore ratio  $de$  is proportional to the change in water ratio  $de_w$  and that the proportionality is controlled by the scaling factor  $f_c(S_r)$ .  $f_c(S_r)$  is a function of the degree of saturation  $S_r$ . The relationship between the change in void ratio  $de$  and the change in water ratio  $de_w$  can be expressed as

$$de_w = f_c(s_r)de \tag{2}$$

The relationship between the void ratio and the water ratio is

$$e_w = S_r e \tag{3}$$

Therefore, Eq. (2) also has to satisfy two limit states, the soil being completely dry ( $S_r=0$ ) and saturated ( $S_r=1$ ). When  $S_r=0$ , no water is present in the soil and a change in the void ratio does not cause any change in the water ratio; therefore,  $f_c(0)=0$ . When  $S_r=1$ , the pores are completely filled with water and a change in the void ratio causes the same change in the water ratio, hence  $f_c(1)=1$ . When the soil is partially saturated ( $0 < S_r < 1$ ), the change in void ratio  $de$  causes a proportional change in the water ratio  $de_w$ . The scaling factor  $f_c(S_r)$  is referred to here as the "coupling function" and the coupling function does not depend on the matric suction.

From Eq. (3), it follows that

$$de_w = S_r de + e dS_r \tag{4}$$

Substituting Eq. (4) into Eq. (2), we can get:



$$dS_r = g_c \frac{de}{de} \tag{5}$$

where  $g_c(S_r) = f_c(S_r) - S_r$ . The physical meaning of Eq. (5) is that at the same degree of saturation, the change in saturation is related to the rate of change in the void ratio, but not to the void ratio.

According to the principle of suction equilibrium, as the suction decreases the water always tends to fill the smaller pore sizes first. Conversely, as the suction increases, the water tends to drain out of the larger pores first. Therefore, for a given suction level, there is a critical pore diameter and the pores in the soil with a pore diameter less than or equal to the critical pore diameter are saturated, while the pores larger than the critical pore diameter are filled with air. The difference between empty pores and saturated pores is mainly in the pore diameter. However, soil deformation is a direct influence on pore diameter. The structural strength of soils during deformation is mainly derived from the strength and number of particles contact points per unit volume (Li et al. 2019). With the increase of pore diameter, the contact point of particles in unit volume decreases, so soil compression tends to start from larger diameter pores (Wang et al. 2021a). Therefore, the change in pore diameter depends mainly on the pressure level. When the pressure is low, if the pore diameter generated by macropore compression is still larger than the critical pore diameter, the empty pore will not be transformed into saturated pore (Wang et al. 2021a). When the pressure is high, the empty pore and saturated pore are compressed simultaneously. When the pressure is moderate, if the pore diameter generated by the compression of macropores is smaller than the critical pore diameter, the transformation of empty pore to saturated pore (Xu et al. 2021a, b). Here, we present two assumptions to illustrate the possible mathematical form of the coupling function based on the possible deformation patterns of the pores. The first assumption is that the change in pore volume caused by compression or expansion of the soil under constant suction does not change the saturated state of the pores, i.e., the saturated pores remain saturated before and after deformation and the air-filled pores remain in a dry state. The second assumption is that the pore saturation state changes when the soil is deformed under constant suction, i.e., pores initially filled with air have the potential to become saturated during the deformation process.

For the first assumption, the deformation of the soil under constant suction does not change the saturation states of the pores, and therefore, the water ratio can only change through compression or expansion of the saturated pores. Based on this assumption we consider two possible mechanisms of extreme deformation.

The first mechanism is that a change in pore ratio at constant suction will only change the larger sized pores, while

the smaller sized saturated pores are not affected. Therefore, the water ratio does not change when the soil has not reached full saturation ( $0 \leq S_r < 1$ ), i.e.,  $de_w/de = 0$ . When the soil is saturated,  $de_w/de = 1$ . Thus, the expression for the coupling function is

$$\begin{cases} f_c(S_r) = 0 & 0 \leq S_r < 1 \\ f_c(S_r) = 1 & S_r = 1 \end{cases} \tag{6}$$

Equation (6) still satisfies two limiting conditions, namely,  $f_c(0) = 0$  and  $f_c(1) = 1$ .

The second mechanism is that the saturated pores and the pores filled with air in a volume deformation under constant suction produce the same proportion of change. The water ratio and the void ratio have the same rate of change, i.e.,  $de_w/e_w = de/e$ . From  $de_w/de = e_w/e = S_r$ , the coupling function is equal to the saturation at this point:

$$f_c(S_r) = S_r \tag{7}$$

Equation (7) indicates that the volume change does not cause a change in the degree of saturation at a constant suction. In addition, Eq. (7) satisfies the two limiting conditions of complete drying and saturation, i.e.,  $f_c(0) = 0$  and  $f_c(1) = 1$ .

The two mechanisms represent two extreme cases and do not have universal applicability. Under low degree of saturation, the soil compression has a greater effect on the empty pore and the water within the saturated pore hardly drains. In this case, the specimen compression is closer to the first mechanism, i.e., the coupling function tends to Eq. (6). Conversely, at higher degrees of saturation, specimen compression also causes deformation of partially saturated pores. In this case, the specimen compression is closer to the second mechanism, i.e., the coupling function tends to Eq. (7). Combining the above two mechanisms and considering the situation between the two extreme mechanisms, the coupling function can be improved as

$$f_c(S_r) = S_r^a \tag{8}$$

where  $a$  is the model parameter. To satisfy the two limiting conditions of complete drying and saturation, i.e.,  $f_c(0) = 0$  and  $f_c(1) = 1$ , Eq. (8) must control  $a > 0$ . In addition, limit  $a \geq 1$  to avoid coupling functions larger than degree of saturation. Because the coupling function once greater than the degree of saturation has the following equation:

$$de_w/de > S_r \Rightarrow de_w/e_w > de/e \tag{9}$$

The physical meaning of Eq. (9) is that the rate of change of water ratio is greater than the rate of change of pore, which is obviously not valid during the actual deformation of the soil. In addition, when the parameter  $a$  tends to infinity, Eq. (8) can be simplified to Eq. (6). When the parameter  $a$  is

equal to 1, then it simplifies to Eq. (7). The two mechanisms are special cases of Eq. (8).

The first assumption, although useful for understanding the deformation behavior of soils, is not realistic in soil deformation. Therefore, the second assumption is that the saturation state of individual pores changes during deformation under constant suction, and the volume change may also lead to water discharge from saturated pores or water absorption saturation of empty pores. According to the Young–Laplace equation, the maximum saturated pore size and the suction are inversely proportional. Under constant suction, the pores larger than this pore diameter are filled with air, and the pores smaller than this pore diameter are in saturation. The pore size decreases when the soil is compressed, and when the smallest empty pore diameter is less than or equal to the maximum saturated pore diameter, these pores will absorb water and become saturated. Conversely, some saturated pores are larger than the maximum saturated pore size due to expansion, and these voids will drain into empty pores. The water ratio decreases as the void ratio increases and increases as the void ratio decreases (Buenfil et al. 2005; Sivakumar 1993). In summary in this mechanism, the change in void ratio produces a change in water ratio opposite to its sign. Therefore, the mathematical form of the coupling function must be flexible enough to obtain positive and negative values depending on the saturation. One expression that meets this condition is

$$f_c(S_r) = b_1 S_r^a + b_2 S_r \tag{10}$$

where  $a$ ,  $b_1$  and  $b_2$  are the model parameters,  $b_1 + b_2 = 1$ . Equation (10) can be simplified to Eq. (8) when  $b_1 = 1$ , so  $a \geq 1$ . From Eq. (9), to ensure that the coupling function is less than the degree of saturation, it is necessary to also ensure that  $b_1 > 0$ . Equation (10) also satisfies the two limiting conditions of complete drying and saturation, i.e.,  $f_c(0) = 0$  and  $f_c(1) = 1$

Bringing Eq. (9) into Eq. (3), expressing the saturation with water ratio and void ratio:

$$de_w/de = b_1(e_w/e)^a + b_2(e_w/e) \tag{11}$$

Integrating Eq. (11), the relationship between water ratio and void ratio at constant suction is obtained as follows:

$$e_w(e, \psi) = [e^{a-1} / (1 + C(\psi)e^{b_1(a-1)})]^{1/(a-1)} \tag{12}$$

where  $\psi$  is the matric suction;  $C(\psi)$  is the integration constant, whose magnitude depends on the matric suction.

By dividing both the left and right sides of the equation by the void ratio, the water ratio can be expressed in terms of the degree of saturation:

$$S_r(e, \psi) = [1 / (1 + C(\psi)e^{b_1(a-1)})]^{1/(a-1)} \tag{13}$$

The integration constant  $C(\psi)$  dependent on the suction is difficult to calculate directly, but can be replaced by a feasible isovolumetric retention curve.

The isochoric retention curve describes the variation of saturation with matric suction when the pore ratio is constant, so the relationship between  $C(\psi)$  and the isochoric retention curve is obtained by setting  $e = e_0$ .

$$C(\psi) = [1/S_r^{a-1}(e_0, \psi) - 1] / e_0^{b_1(a-1)} \tag{14}$$

Substituting Eq. (14) into Eq. (13), the integration constant, can be eliminated:

$$S_r(e, \psi) = \left\{ 1 / \left[ 1 + (1/S_r^{a-1}(e_0, \psi) - 1)(e/e_0)^{b_1(a-1)} \right] \right\}^{1/(a-1)} \tag{15}$$

Equation (15) describes the combined effect of suction and void ratio on the degree of saturation. Using Eq. (15) to describe the effect of void ratio and suction on degree of saturation can be done in two steps. The first step is to select the isovolumetric retention curve model  $S_r(e_0, \psi)$ . Among the isovolume retention curves, a large number of research results have been published, among which the most commonly used are the VG model and the Fredlund–Xing model (Fredlund and Xing 1994; van Genuchten 1980). The model is selected and the isovolumetric retention curve parameters are obtained by fitting the matric suction and degree of saturation data under isovolumetric conditions. In the second step, the obtained isovolumetric retention curves are brought into Eq. (15) and then the deformation data (void ratio and degree of saturation) at constant suction are fitted to obtain the parameters  $a$  and  $b_1$ .

### Unsaturated permeability model

In the steady flow state Darcy's theorem also applies to unsaturated infiltration (Tian et al. 2020), which is known from Darcy's theorem:

$$k = \frac{Q}{Ai} \tag{16}$$

where  $k$  is the permeability coefficient;  $A$  is the sectional area of the sample;  $Q$  is the sample volume flow rate;  $i$  is the hydraulic gradient.

Because the soil is composed of massive, connected pores, seepage occurs in these connected pores. In addition, unsaturated soil always fills smaller pores size during humidification. Due to the attenuation of matric suction, water gradually moves into the macropores. Therefore, integration can be used to divide the pores into  $n$  grades based on the pore size. It is assumed that only the first  $m$  classes of pores are filled with water under constant matric suction. Therefore, the pore flow

$Q$  of the sample can be expressed as the sum of the pore volume flow of the first  $m$  grades ( $m \leq n$ ):

$$Q = \sum_{i=1}^m q_i \tag{17}$$

According to Hagen Poiseuille, the volume flow  $q_i$  in the pores of grade  $i$  can be expressed as

$$q_i = \frac{\pi r_i^4 \Delta p}{8 \eta l} \tag{18}$$

where  $q_i$  is the volume flow of the  $i$ th grade pore;  $r_i$  is the pore radius;  $\Delta p$  is the pressure difference between the two ends of the pore;  $\eta$  is the viscosity coefficient;  $l$  is the pore length. Assuming that the ratio of pore length ( $l$ ) to sample length ( $L$ ) is  $p_i$ , the pore length can be expressed as  $L p_i$ .

Therefore, formula (16) can be expressed as

$$k = \frac{\sum_{i=1}^m \frac{\pi r_i^4 \Delta p}{8 \eta l}}{A_i} \tag{19}$$

Due to the  $i$ -grade pore cross-sectional area  $A_i = \pi r_i^2$ ; head loss  $\Delta h = \Delta p / \rho g$ ;  $i = \Delta h / L$ . Therefore, Eq. (19) can be expressed as

$$k = \frac{\rho g}{8 \eta A} \sum_{i=1}^m \frac{r_i^2 A_i}{p_i} \tag{20}$$

The volume of liquid in the  $i$ th pore is  $\Delta V_w$ . Therefore,  $\Delta V_w = A_i L p_i$ ; therefore, Eq. (20) can be further expressed as

$$k = \frac{\rho g}{8 \eta A} \sum_{i=1}^m \frac{r_i^2 \Delta V_w}{p_i^2} \tag{21}$$

where  $V$  is the sample volume.

For an ideal pore model,  $p_i$  can be assumed to be a constant (Tao and Kong 2017). Therefore, the above formula can be written as

$$k = k_c \sum_{i=1}^m \frac{r_i^2 \Delta V_w}{V} \tag{22}$$

where  $k_c = \rho g / 8 \eta p_i^2$ . For the same soil  $k_c$  is a constant.

The Young–Laplace equation was introduced to explain the influence of large pores on the inlet value, as

$$\psi_i = \frac{4 T_s \cos \alpha}{d_i} \tag{23}$$

where  $d_i$  is the  $i$ th pore diameter;  $\psi_i$  is the matric suction corresponding to  $d_i$ ;  $T_s$  is the surface tension on the water–gas interface, when the temperature is 30 °C,  $T_s = 71.42$  kN/m (Wang et al. 2021b, c); and  $\alpha$  is the contact angle between soil particles and pore water, generally being 0°.

To relate the permeability model to the SWRC model, the water volume is converted to degree of saturation.

$$\frac{\Delta V_w}{V} = \frac{e}{1+e} \Delta S_r \tag{24}$$

Bringing Eqs. (23) and (24) into Eq. (22) can relate the permeability coefficient to matric suction and degree of saturation:

$$k(S_r, e) = k_d \frac{e}{1+e} \sum_{i=1}^m \frac{\Delta S_r}{\psi_i^2} \tag{25}$$

where  $k_d = (2 T_s \cos \alpha)^2 k_c$ . For the same soil in the same test conditions  $k_d$  is a constant.

When using Eq. (25) for unsaturated permeability coefficient calculation, the specific steps are: based on the SWRCs with different void ratios obtained with Eq. (15), a SWRC with a selected void ratio is divided into  $n$  segments according to the degree of saturation (Fig. 4). The amount of saturation change at level  $i$  is  $\Delta S_r$ , and the median value of saturation at section  $i$  corresponds to the matric suction of  $\psi_i$ . The  $n$ -segment data (degree of saturation and matric suction), the pore ratio and the saturation permeability coefficient measured by saturation permeability are brought into Eq. (25) to obtain the constant  $k_d$ . Assuming that only the first  $m$  levels of pores are saturated, the unsaturated permeability coefficient can be found by bringing the first  $m$  levels  $\Delta S_r$  and  $\psi_i$  into Eq. (25) if  $k_d$  is known.

Since Eq. (15) can be derived as the expression of SWRCs for specimens with different void ratios, Eq. (25) is written in integral form as

$$k(S_r, e) = k_d \frac{e}{1+e} \int_0^{S_r} \frac{dS_r}{\psi^2(S_r, e)} \tag{26}$$

The permeability coefficient when the specimen is saturated ( $S_r = 1$ ) is

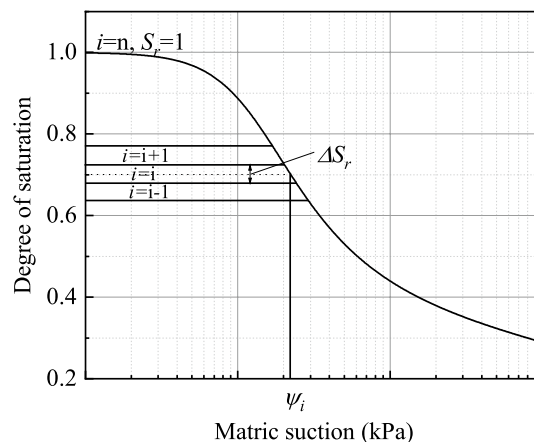


Fig. 4 Soil water retention curve differential intent

$$k_s(e) = k_d \frac{e}{1+e} \int_0^1 \frac{dS_r}{\psi^2(S_r, e)} \tag{27}$$

The relative permeability coefficient can be expressed as

$$k_r(S_r, e) = \frac{\int_0^{S_r} \frac{dS_r}{\psi^2(S_r, e)}}{\int_0^1 \frac{dS_r}{\psi^2(S_r, e)}} \tag{28}$$

The relative permeability coefficient is calculated as follows: after solving the expression of SWRC with different void ratios in Eq. (15), the expression is brought into Eq. (28) to find the relative permeability coefficient of specimens with different pore ratios at different degrees of saturation. If you solve the unsaturated permeability coefficient, you first need to solve for the constant  $k_d$ . Saturated permeability test is performed on any of the void ratio specimens to obtain the saturation permeability coefficient. The void ratio, saturation permeability coefficient and the SWRC at this void ratio are brought into Eq. (27) to obtain the constant  $k_d$ . The permeability coefficients of specimens with different void ratios and different degrees of saturation can be obtained by bringing the constant  $k_d$  and the expression of SWRC with different void ratios into Eq. (26).

## Results and model validation

### SWRC model validation

Moisture and water potential sensors buried at the same location in the soil column provide real-time measurements of volumetric moisture content and matric suction at that point. Various models have been proposed by domestic and foreign scholars to reflect the relationship between water content and matric suction. In this paper, the Fredlund–Xing model is used as the constant volume SWRC model. Because the medium-volume SWRC in Eq. (15) is a curve describing the relationship between matric suction and degree of saturation at a constant void ratio, the volumetric water content is converted to degree of saturation as follows:

$$S_r = \frac{C'(\psi)}{\{\ln [e+(\psi/a)^n]\}^m} \tag{29}$$

$$C'(\psi) = 1 - \frac{\ln(1+\psi/\psi_r)}{\ln(1+10^6/\psi_r)} \tag{30}$$

where  $C'(\psi)$  is the correction factor;  $\psi_r$  is the matric suction corresponding to the residual water content, generally taken as  $\psi_r = 3000\text{kPa}$  (Sillers et al. 2001); and  $e$  is the natural constant.

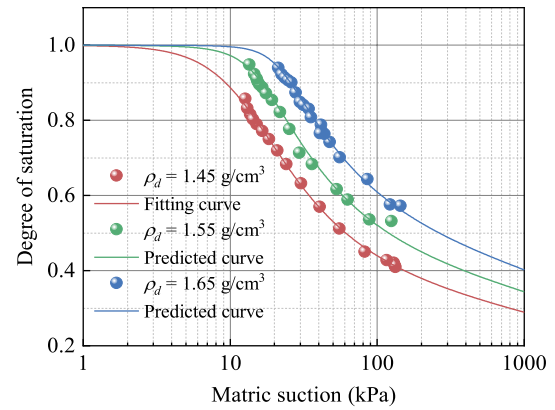


Fig. 5 Fitted and predicted isochoric SWRCs

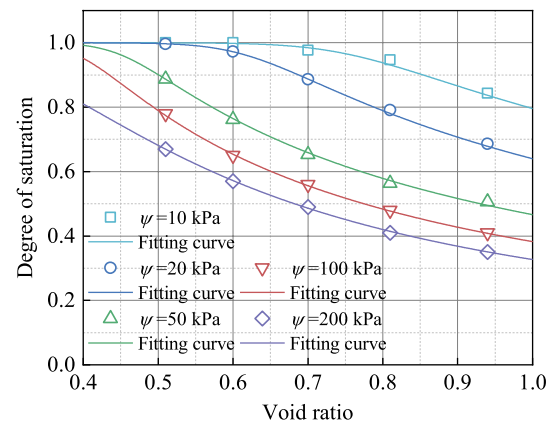


Fig. 6 Relationship curve between void ratio and degree of saturation under constant suction

As seen in Sect. “SWRC model considering deformation”, after selecting the constant volume retention curve, a constant volume retention curve model is used to fit the data. In this paper, the Fredlund–Xing model (Eq. (29)) was first used to fit the matric suction–saturation of the 1.45 g/cm<sup>3</sup> soil column at this point  $e_0 = 0.87$  (Fig. 5). The fitted curves are in good agreement with the measured data, and the correlation coefficient  $R^2$  is 0.998, indicating that the model fits the water retention curve of compacted loess in this study very well. The parameters in Eq. (29) were obtained by fitting, so that the constant volume retention curve is

$$S_r(0.87, \psi) = \frac{C'(\psi)}{\{\ln [e+(\psi/11.16)^{2.15}]\}^{0.52}} \tag{31}$$

Equation (31) is brought into Eq. (15) and then deformation data (void ratio and degree of saturation) at constant suction are fitted to obtain parameters  $a$  and  $b_1$ . Wang et al. (2021c) examined the gravimetric water content of Yan'an



**Table 2** Model parameters

Suction (kPa)	Parameter		$R^2$
	$a$	$b_1$	
10	13.87	1.02	0.966
20	16.66	0.95	0.996
50	16.87	0.97	0.997
100	14.84	1.05	0.998
200	12.85	1.04	0.999
Mean	15.018	1.006	–

compacted loess specimens with varying dry densities under constant matric suction. To align with the objectives of our study, we transformed the dry density into void ratio and the gravimetric water content into saturation, as depicted in Fig. 6. Equation (31) was brought into Eq. (15) and the experimental data were fitted according to the least squares method, where the void ratio was used as the independent variable and the degree of saturation as the dependent variable (Fig. 6). The fitted parameters for the two suctions are summarized in Table 2. The  $R^2$  was all greater than 0.966 and the fitted parameters were very close at different suction, indicating that the experiments were in good agreement at different suction, thus confirming the ability of the model to predict the degree of saturation of soils with different pore ratios at different suction. Therefore, the average value of the parameters at different suction is taken as the final value of the parameters.

The mean values of parameters  $a$  and  $b_1$  are brought into Eq. (14), at which time the expression of the Yan'an loess SWRC is.

$$S_r(e, \psi) = \left\{ 1 + \left( \left( \frac{\ln(2.72 + (\psi/11.16)^{2.15})^{0.52}}{C'(\psi)} \right)^{14.018} - 1 \right) \left( \frac{e}{0.87} \right)^{14.1} \right\}^{-0.071} \tag{32}$$

To verify the accuracy of Eq. (31), the matric suction and saturation obtained for the 1.55 and 1.65 g/cm<sup>3</sup> soil columns were predicted (Fig. 6). Figure 6 shows that the measured and predicted degrees of saturation for different dry densities under different suction are in general agreement. This illustrates that Eq. (32) has the capability to predict the degree of saturation of Yan'an compacted loess under deformation conditions. In addition, it demonstrates that the SWRC model in Eq. (15) possesses a degree of practicality in the context of deformation in loess. It is worth noting that Eq. (32) specifically applies this model to compacted loess soil and employs parameters sourced exclusively from Yan'an compacted loess. As a result, the applicability of Eq. (32) may be limited to Yan'an compacted loess. The suitability of this equation to other soil types is an area for further investigation.

## Validation of permeability coefficient prediction model

### Prediction of saturation permeability coefficient

The saturation permeation of different dry density specimens can be obtained according to the saturation permeation test (Table 3). Take 1.45 g/cm<sup>3</sup> dry density specimen as an example, bring Eq. (32) into Eq. (27), and then use the saturation permeability coefficient and void ratio obtained from the test to find the constant  $k_d = 0.018$ . The steps of predicting the saturated permeability coefficients of other samples with void ratios are similar to the above steps. First, Eq. (32) is brought into Eq. (27), and then put the obtained constants  $k_d$  and void ratios into equations to obtain the saturation permeability coefficients of specimens with different void ratios (Table 3). It can be seen that the predicted values have some deviations compared with the tested values, but they are of the same order of magnitude, indicating that the model proposed in this paper can be used for the prediction of saturated permeability coefficients of the compacted loess in Yan'an.

### Prediction of unsaturated permeability coefficient

During infiltration, the total head  $h_w$  at any position  $z_j$  without considering the osmotic pressure head is equal to the sum of the position head  $z_j$  and the matric suction head  $h_m$ , which is

$$h_w = z_j + h_m \tag{33}$$

The hydraulic gradient  $i_w$  at point  $z_j$  at time  $t$  is equal to the slope of the head distribution line at that point, which is

$$i_w = \frac{h_w}{dz} \tag{34}$$

The water volume  $V_w$  between point  $z_j$  and the top of the soil column is

**Table 3** Test value and predicted value of saturated permeability coefficient

$\rho_d$ (g/cm <sup>3</sup> )	1.45	1.55	1.65
Test $k_s$ (cm/s)	$1.18 \times 10^{-4}$	$6.14 \times 10^{-5}$	$2.35 \times 10^{-5}$
Predicted $k_s$ (cm/s)	–	$2.83 \times 10^{-5}$	$1.18 \times 10^{-5}$

$$V_w = \int_0^{z_j} \theta_w(z)_t Adz \tag{35}$$

where  $A$  is the cross-sectional area of the soil column ( $\text{cm}^2$ );  $\theta_w(z)_t$  is the volumetric water content at point  $z$  at time  $t$ .

The flow velocity  $v_w$  at point  $z_j$  can be expressed as

$$v_w = \frac{dV_w}{Adt} \tag{36}$$

The unsaturated permeability coefficient is

$$k = -\frac{v_m}{i_{ave}} \tag{37}$$

where  $i_{ave}$  is the average hydraulic gradient of the point within the selected time.

The forward difference method is used when calculating  $i_{ave}$ , which is

$$i_{ave} = \frac{1}{2} \left( \frac{h_{w(j+1),t1} - h_{w(j),t1}}{z_{j+1} - z_j} + \frac{h_{w(j+1),t2} - h_{w(j),t2}}{z_{j+1} - z_j} \right) \tag{38}$$

where  $h_{w(j),t}$  is the water head at point  $z_j$  at time  $t$ .

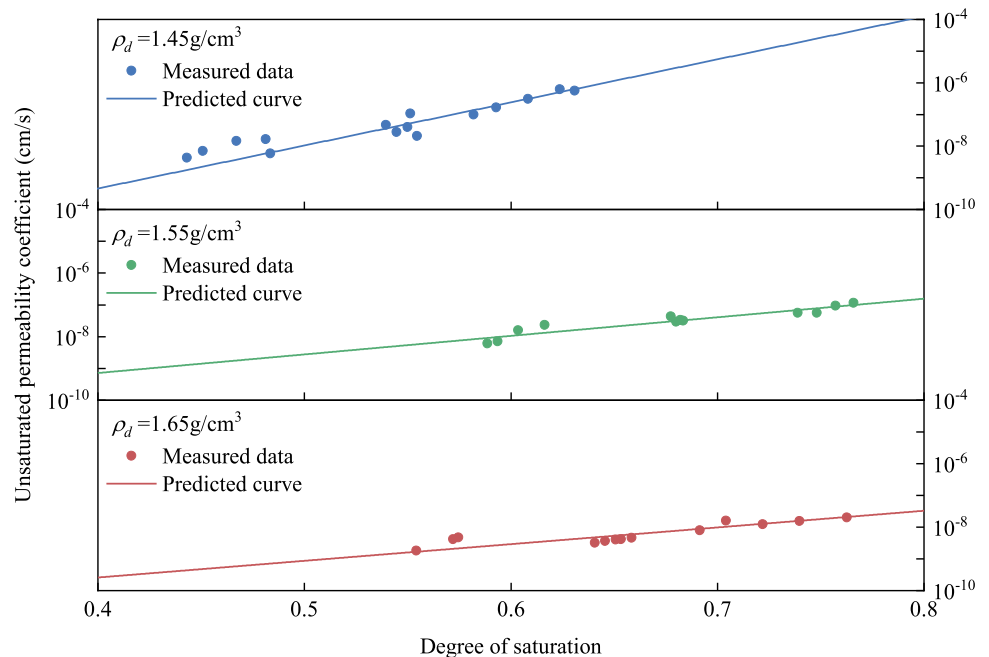
According to the volumetric water content and matric suction monitored using the MPS-6 water potential sensor and EC-5 water sensor, the relationship between the unsaturated permeability coefficient and degree of saturation of compacted loess with different dry densities can be calculated using the instantaneous profile method (Fig. 7). The unsaturated permeability coefficient prediction method is basically the same as the saturated permeability coefficient

prediction method. First, the formula (32) is brought into the formula (26), and then the constant and void ratio obtained above are brought into the formula (26) to obtain the relationship curves between degree of saturation and unsaturated permeability coefficient for different pore ratios (Fig. 7). To verify the accuracy of the model, the experimental data and predicted unsaturated permeability coefficient curve are plotted on the same graph (Fig. 7).

Figure 7 shows that the measured and predicted values of unsaturated permeability coefficient are in general agreement. It shows that for Yan'an compacted loess in a certain state, where the void ratio and saturated permeability coefficient are known, the saturated/unsaturated permeability coefficient of any pore ratio specimen can be predicted by following the above steps.

It should be noted that Eqs. (15) and (26) can in theory predict SWRCs and unsaturated permeability coefficients for any soil under deformation conditions, but the data used in the validation process of this paper are from the compacted loess of Yan'an New District. Therefore, the parameters in Sect. "Results and model validation" can only guarantee the applicability to Yan'an loess, and the applicability to other types of soils needs to be further verified. For the use of other soils refer to the use methods in Sect. "Results and model validation". In summary, the prediction model proposed in this paper is simple, reliable and practical, and can provide technical support for the study of unsaturated soil seepage during deformation.

**Fig. 7** Measured unsaturated permeability coefficient and the corresponding prediction curve



## Conclusions

In this paper, the SWRC model and the unsaturated infiltration model were established under the consideration of deformation conditions, and the reliability of the models was verified. The following conclusions are mainly obtained:

1. In this paper, a coupling function is set to link the change of water ratio with the change of void ratio under constant suction. The coupling function contains two parameters that extend the traditional isochoric SWRCs to different void ratio states. The SWRCs with different void ratios can be predicted by the model proposed in this paper.
2. Darcy's theorem is still applicable to unsaturated seepage. First, the pore size distribution is differentiated to propose a permeability coefficient model based on the pore size distribution, furthermore, the pore size distribution is transformed into a SWRC. Finally, the saturated/unsaturated permeability coefficient prediction model considering soil deformation is derived by means of the SWRC considering the deformation.
3. The SWRC model and the permeability coefficient prediction model were verified using the measured data. The SWRC model can accurately describe not only the SWRC of constant-volume soils, but also the SWRC with different void ratios; the permeability coefficient prediction model can also accurately predict the permeability coefficient of Yan'an compacted loess.
4. This model not only considers the effects of void ratio and suction on the degree of saturation, but also considers the effects of void ratio and saturation on the permeability coefficient, so it can provide some support for the study of water-force coupling in unsaturated soils.

**Author contributions** HW and KY wrote the main manuscript text. All authors reviewed the manuscript.

**Funding** This study was financially supported by the National Nature Science Foundation of China (Grant no. 41931285) and the key research and development program of Shaanxi Province (Grant no. 2020SF-436; 2019ZDLSF05-07).

**Data availability** Some or all data, models, or codes that support the findings of this study are available from the corresponding author upon reasonable request.

## Declarations

**Conflict of interest** The authors declare no competing interests.

## References

- Agus SS, Leong E-C, Rahardjo H (2005) Estimating permeability functions of Singapore residual soils. *Eng Geol* 78:119–133. <https://doi.org/10.1016/j.enggeo.2004.12.001>
- Beckett CTS, Augarde CE (2013) Prediction of soil water retention properties using pore-size distribution and porosity. *Can Geotech J* 50:435–450. <https://doi.org/10.1139/cgj-2012-0320>
- Buenfil C, Romero E, Lloret A, Gens A (2005) Hydro-mechanical behaviour of a clayey silt under isotropic compression. In: Schanz T (ed) *Unsaturated soils: experimental studies*. Springer, Berlin Heidelberg, pp 331–342
- Da S, Sheng D, Sloan SW (2007) Elastoplastic modelling of hydraulic and stress–strain behaviour of unsaturated soils. *Mech Mater* 39:212–221. <https://doi.org/10.1016/j.mechmat.2006.05.002>
- Fredlund DG, Xing A (1994) Equations for the soil-water characteristic curve. *Can Geotech J* 31:521–532. <https://doi.org/10.1139/t94-061>
- Frydman S, Baker R (2009) Theoretical soil-water characteristic curves based on adsorption, cavitation, and a double porosity model. *Int J Geomech* 9:250–257. [https://doi.org/10.1061/\(ASCE\)1532-3641\(2009\)9:6\(250\)](https://doi.org/10.1061/(ASCE)1532-3641(2009)9:6(250))
- Gallipoli D (2012) A hysteretic soil-water retention model accounting for cyclic variations of suction and void ratio. *Géotechnique* 62:605–616. <https://doi.org/10.1680/geot.11.P.007>
- Gallipoli D, Wheeler SJ, Karstunen M (2003) Modelling the variation of degree of saturation in a deformable unsaturated soil. *Géotechnique* 53:105–112. <https://doi.org/10.1680/geot.2003.53.1.105>
- Gardner W (1958) Mathematics of isothermal water conduction in unsaturated soils. *Highw Res Board Spec Rep* 40:78–87
- Gens A, Valleján B, Sánchez M, Imbert C, Villar MV, Geet MV (2011) Hydromechanical behaviour of a heterogeneous compacted soil: experimental observations and modelling. *Géotechnique* 61:367–386. <https://doi.org/10.1680/geot.SIP11.P.015>
- Gui M-W, Hsu C-S (2009) Generalized fitting parameters of three permeability functions for predicting water coefficient of permeability of lateritic soil. *Geotech Test J* 32:418–427. <https://doi.org/10.1520/GTJ101931>
- Hu R, Chen Y-F, Liu H-H, Zhou C-B (2013) A water retention curve and unsaturated hydraulic conductivity model for deformable soils: consideration of the change in pore-size distribution. *Géotechnique* 63:1389–1405. <https://doi.org/10.1680/geot.12.P.182>
- Huang S, Barbour SL, Fredlund DG (1998) Development and verification of a coefficient of permeability function for a deformable unsaturated soil. *Can Geotech J* 35:411–425. <https://doi.org/10.1139/t98-010>
- Hunt AG, Ghanbarian B, Saville KC (2013) Unsaturated hydraulic conductivity modeling for porous media with two fractal regimes. *Geoderma* 207–208:268–278. <https://doi.org/10.1016/j.geoderma.2013.05.023>
- Iyer KKR, Joseph J, Lopes BCFL, Singh DN, Tarantino A (2018) Water retention characteristics of swelling clays in different compaction states. *Geomech Geoeng* 13:88–103. <https://doi.org/10.1080/17486025.2017.1396363>
- Iyer KKR, Shetty R, Joseph J, Singh DN (2019) Influence of microstructure on drying- and wetting-characteristics of fine-grained soils. *Geomech Geoeng* 14:271–284. <https://doi.org/10.1080/17486025.2019.1597283>
- Lebeau M, Konrad J-M (2010) A new capillary and thin film flow model for predicting the hydraulic conductivity of unsaturated porous media. *Water Resour Res*. <https://doi.org/10.1029/2010WR009092>

- Leong E-C (2019) Soil-water characteristic curves—determination, estimation and application. *Jpn Geotech Soc Spec Publ* 7:21–30. <https://doi.org/10.3208/jgssp.v07.003>
- Li P, Li T-l, Vanapalli SK (2018) Prediction of soil–water characteristic curve for Malan loess in Loess Plateau of China. *J Central South Univ* 25:432–447. <https://doi.org/10.1007/s11771-018-3748-1>
- Li P, Xie W, Pak RYS, Vanapalli SK (2019) Microstructural evolution of loess soils from the Loess Plateau of China. *CATENA* 173:276–288. <https://doi.org/10.1016/j.catena.2018.10.006>
- Mašín D (2010) Predicting the dependency of a degree of saturation on void ratio and suction using effective stress principle for unsaturated soils. *Int J Numer Anal Meth Geomech* 34:73–90. <https://doi.org/10.1002/nag.808>
- Monroy R, Zdravkovic L, Ridley A (2010) Evolution of microstructure in compacted London Clay during wetting and loading. *Géotechnique* 60:105–119. <https://doi.org/10.1680/geot.8.P.125>
- Mu QY, Dong H, Liao HJ, Dang YJ, Zhou C (2020) Water-retention curves of loess under wetting–drying cycles. *Géotech Lett* 10:135–140. <https://doi.org/10.1680/jgele.19.00025>
- Muñoz-Castelblanco JA, Pereira JM, Delage P, Cui YJ (2012) The water retention properties of a natural unsaturated loess from northern France. *Géotechnique* 62:95–106. <https://doi.org/10.1680/geot.9.P.084>
- Ng CWW, Sadeghi H, Hossen SKB, Chiu CF, Alonso EE, Baghbarezvan S (2016) Water retention and volumetric characteristics of intact and re-compacted loess. *Can Geotech J* 53:1258–1269. <https://doi.org/10.1139/cgj-2015-0364>
- Nuth M, Laloui L (2008) Advances in modelling hysteretic water retention curve in deformable soils. *Comput Geotech* 35:835–844. <https://doi.org/10.1016/j.compgeo.2008.08.001>
- Otalvaro IF, Neto MPC, Delage P, Caicedo B (2016) Relationship between soil structure and water retention properties in a residual compacted soil. *Eng Geol* 205:73–80. <https://doi.org/10.1016/j.enggeo.2016.02.016>
- Oualmakran M, Mercatoris BCN, François B (2016) Pore-size distribution of a compacted silty soil after compaction, saturation, and loading. *Can Geotech J* 53:1902–1909. <https://doi.org/10.1139/cgj-2016-0184>
- Pasha Amin Y, Khoshghalb A, Khalili N (2016) Pitfalls in interpretation of gravimetric water content-based soil–water characteristic curve for deformable porous media. *Int J Geomech* 16:D4015004. [https://doi.org/10.1061/\(ASCE\)GM.1943-5622.0000570](https://doi.org/10.1061/(ASCE)GM.1943-5622.0000570)
- Reicosky DC, Voorhees WB, Radke JK (1981) Unsaturated water flow through a simulated wheel track. *Soil Sci Soc Am J* 45:3–8. <https://doi.org/10.2136/sssaj1981.03615995004500010001x>
- Romero E, Jommi C (2008) An insight into the role of hydraulic history on the volume changes of anisotropic clayey soils. *Water Resour Res*. <https://doi.org/10.1029/2007WR006558>
- Sillers WS, Fredlund DG, Zakerzadeh N (2001) Mathematical attributes of some soil–water characteristic curve models. In: Toll DG (ed) *Unsaturated soil concepts and their application in geotechnical practice*. Springer, Dordrecht, pp 243–283
- Tao G, Wu X, Xiao H, Chen Q, Cai J (2019) A unified fractal model for permeability coefficient of unsaturated soil. *Fractals* 27:1940012. <https://doi.org/10.1142/s0218348x19400127>
- Tian K, Yang A, Nie K, Zhang H, Xu J, Wang X (2020) Experimental study of steady seepage in unsaturated loess soil. *Acta Geotech* 15:2681–2689. <https://doi.org/10.1007/s11440-020-00948-2>
- van Genuchten MT (1980) A closed-form equation for predicting the hydraulic conductivity of unsaturated soils. *Soil Sci Soc Am J* 44:892–898. <https://doi.org/10.2136/sssaj1980.03615995004400050002x>
- Wang H-m, Ni W-k, Yuan K-z, Li L, Nie Y-p, Guo Y-x (2021a) Microstructure evolution of loess under multiple collapsibility based on nuclear magnetic resonance and scanning electron microscopy. *J Mt Sci* 18:2612–2625. <https://doi.org/10.1007/s11629-021-6838-8>
- Wang H, Ni W, Li X, Li L, Yuan K, Nie Y (2021b) Predicting the pore size distribution curve based on the evolution mechanism of soil–water characteristic curve. *Environ Earth Sci* 81:23. <https://doi.org/10.1007/s12665-021-10138-2>
- Wang Y, Li T, Zhao C, Hou X, Li P, Zhang Y (2021c) A study on the effect of pore and particle distributions on the soil water characteristic curve of compacted loess soil. *Environ Earth Sciences* 80:764. <https://doi.org/10.1007/s12665-021-09973-0>
- Wen T, Shao L, Guo X, Zhao Y, Huang L, Chen X (2019) Error correction of water evaporation loss on the unsaturated hydraulic conductivity. *Soils Found* 59:2341–2347. <https://doi.org/10.1016/j.sandf.2019.08.015>
- Wen T, Shao L, Guo X, Zhao Y (2020) Experimental investigations of the soil water retention curve under multiple drying–wetting cycles. *Acta Geotech* 15:3321–3326. <https://doi.org/10.1007/s11440-020-00964-2>
- Wen T, Shao L, Guo X (2021a) Permeability function for unsaturated soil. *Eur J Environ Civ Eng* 25:60–72. <https://doi.org/10.1080/19648189.2018.1515666>
- Wen T, Wang P, Shao L, Guo X (2021b) Experimental investigations of soil shrinkage characteristics and their effects on the soil water characteristic curve. *Eng Geol* 284:106035. <https://doi.org/10.1016/j.enggeo.2021.106035>
- Wen T, Chen X, Shao L (2022) Effect of multiple wetting and drying cycles on the macropore structure of granite residual soil. *J Hydrol* 614:128583. <https://doi.org/10.1016/j.jhydrol.2022.128583>
- Xu P, Zhang Q, Qian H, Li M, Yang F (2021a) An investigation into the relationship between saturated permeability and microstructure of remolded loess: A case study from Chinese Loess Plateau. *Geoderma* 382:114774. <https://doi.org/10.1016/j.geoderma.2020.114774>
- Yuan K-z, Ni W-k, Lü X-f, Zhu M (2022) Experimental study on the performance of the modified loess by polypropylene fiber mixed with bentonite and cement. *Bull Eng Geol Env* 81:302. <https://doi.org/10.1007/s10064-022-02800-1>
- Zhao Y, Wen T, Shao L, Chen R, Sun X, Huang L, Chen X (2020) Predicting hysteresis loops of the soil water characteristic curve from initial drying. *Soil Sci Soc Am J* 84:1642–1649. <https://doi.org/10.1002/saj2.20125>
- Zhou A-N, Sheng D, Carter JP (2012) Modelling the effect of initial density on soil–water characteristic curves. *Géotechnique* 62:669–680. <https://doi.org/10.1680/geot.10.P.120>
- Sivakumar V (1993) A critical state framework for unsaturated soil. PhD, University of Sheffield
- Tao G, Kong L (2017) A model for determining the permeability coefficient of saturated and unsaturated soils based on micro pore channel and its application. *J Hydraul Eng* 48:702–709. <https://doi.org/10.13243/j.cnki.slx.20160993>
- Xu P, Zhang Q, Qian H, Qu W, Li M (2021b) Microstructure and permeability evolution of remolded loess with different dry densities under saturated seepage. *Eng Geol* 282:105875. <https://doi.org/10.1016/j.enggeo.2020.105875>

**Publisher's Note** Springer Nature remains neutral with regard to jurisdictional claims in published maps and institutional affiliations.

Springer Nature or its licensor (e.g. a society or other partner) holds exclusive rights to this article under a publishing agreement with the author(s) or other rightsholder(s); author self-archiving of the accepted manuscript version of this article is solely governed by the terms of such publishing agreement and applicable law.